Journal of Electroceramics 4:S1, 41–48, 1999


# Oxygen Diffusion in Single- and Poly-Crystalline Zinc Oxides

HAJIME HANEDA, ISAO SAKAGUCHI, AKIO WATANABE, TAKAMASA ISHIGAKI & JUNZO TANAKA
*National Institute for Research in Inorganic Materials, 1-1 Namiki, Tsukuba-shi, Ibaraki 305-0044 Japan*

Submitted November 17, 1997; Revised July 8, 1998; Accepted July 15, 1998

**Abstract.** $^{18}O$ diffusion coefficients were measured in zinc oxide ceramics using a secondary ion mass spectrometer. The results are interpreted as indicating extrinsic behavior. The values of the lattice diffusion coefficients with higher valence dopants compared with zinc ions are greater than lower valence dopant such as lithium ions. Using the data at deeper depth, the grain boundary diffusivity of oxide ions was also evaluated. Although the lattice diffusion coefficients varied by two orders of magnitude, the products of grain boundary width and grain boundary diffusion coefficient were less sensitive to the type of dopants.

**Keywords:** diffusion, oxygen, zinc oxide, grain boundary, dopant, SIMS, interstitial diffusion

## 1. Introduction

Metal-oxide varistors used in surge arresters are ZnO-based ceramic semiconductor devices with highly nonlinear current-voltage characteristics similar to back-to-back Zener diodes, but with much greater current-, voltage, and energy-handling capabilities [1,2]. Such materials are characterized by non-uniform grain size, porosity, second phase distribution, impurity segregation and grain-grain misorientation. The electrical properties of ZnO varistors are, furthermore, known to be greatly influenced by their defect chemistry.

ZnO is known to deviate from stoichiometry. In the case of zinc excess, the point defects can be zinc interstitials or oxygen vacancies. In general, diffusion coefficients, and their temperature and dopant dependence permit conclusions with respect to the transport mechanism and thus to the kind of defect structure. It is generally believed that oxygen ions diffuse via the oxygen vacancy. In this paper, we focus our attention on attempts to investigate diffusion of oxygen ions in various ZnO-based ceramics. We report evidence for an interstitial or interstitialcy mechanism for oxygen diffusion in the ZnO lattice. Furthermore, we also examined oxygen diffusivity along grain boundaries.

## 2. Experimental Procedure

Single crystals were grown by evaporation (Hakusui Chem. Co. Ltd), where the concentration of the major impurity, Al, was less than 10ppm as analyzed by a Cameca magnetic sector type secondary ion mass spectrometer (SIMS, MS-4f) with $O_2^+$ as the primary ions, an accelerating voltage 12.5 kV, and beam current of 10 to 30 nA. The shape of the single crystals was pyramidal with size of a few mm. These were cut along the c axis and basal plane, and then polished to mirror smoothness by diamond pastes of decreasing particle size (10, 3, 1, 0.5 mm). These samples were preannealed in air for an hour at 1073 K, to anneal surface defects.

ZnO based ceramics prepared by a hot-isostatic-pressing were used for oxygen diffusion experiment [3]. Precursor powders were 4N-grade (Hakusui Chem. Co. Ltd). To clarify the doping effect on the oxygen diffusion, Co-, Mn-, Al- and Li-doped samples were used. These powders were pressed at 30 MPa into discs 12 mm in diameter and 6 mm in thickness, and then cold-isostatic pressed at 160 MPa. Thereafter, they were pre-sintered in $O_2$ for 5 h at 1250°C. Porosity became closed after pre-sintering. These discs were treated at 1250°C under an isostaic pressure of 130 MPa in Ar atmosphere without any

capsule, and then annealed in $O_2$ at 1000°C for 5 h. After hipping and annealing, all samples had porosity under 0.2%, and un-doped samples were transparent. This is very favorable since it eliminates the effects of pores during the diffusion experiments. Samples were cut into disks shape. The doping level was fixed at 0.3 at. %. One side of each specimen was polished to optical flatness with diamond paste, following the same procedure as for the single crystals. Polycrystals were not pre-annealed, to limit grain boundary grooving or impurity redistribution along grain boundaries.

Diffusion coefficients were determined by a solid-gas exchange technique [4]. After being cleaned with water, ethanol, acetone, and ethanol, the samples were placed inside a platinum crucible with a platinum susceptor in a vessel of a RF furnace. The system was evacuated and the $^{18}O$-enriched oxygen gas with 5 kPa pressure was introduced into the vessel that was closed from the gas line. The sample crucible was first heated at 700°C for 15 min to maintain the constant concentration at the sample surface, and then the temperature was elevated to a desired temperature for isotope exchange. The temperature was monitored by an optical pyrometer. Although the accuracy of the pyrometer is within 10 K, the temperature variation among samples in the same experimental cycle is believed to be less than a few degrees. After isotopic exchange of oxygen between the gaseous phase and the samples during a given time, the furnace was cooled down by switching off the power and $^{18}O$-enriched gas was re-absorbed back into the zeolite storage flask by trapping with liquid nitrogen.

The $^{18}O$ diffusion profiles (concentration versus depth) were measured using SIMS with $^{133}Cs^+$ as the primary ion, an accelerating voltage of 10 kV, and a beam current of 5 to 20 nA. The primary beam scanned a 100 $\mu$m area, and secondary ion signals were detected within the central 40% part of the sputtered crater. Intensities for the negative ions $^{16}O$ and $^{18}O$ were obtained by an electron multiplier as a function of time. The crater depths were measured using a Dektak 3000 profilometer. For three dimensional analysis, a plannar detector was used (Charze Evans, Co., Resistive anode encoder: RAE). The concentrations of $^{18}O$ are converted as a function of depth., using sputtering duration.

The concentration $(c(x,t))$ of $^{18}O$ at any sample depth, $x$, at diffusion time, $t$, was determined from the ion intensities:

$$c(x,t) = \frac{I(^{18}O)}{I(^{18}O) + I(^{16}O)} \tag{1}$$

where $I(^{18}O)$ and $I(^{16}O)$ are the secondary inrensities of $^{18}O$ and $^{16}O$ isotopes, respectively.

If the surface is maintained at a constant concentration of $^{18}O$, $C_g$, which is the same concentration as in the gaseous phase, and if the concentration in the solid is initially uniform ($C(x,0) = C_0$, natural abundance, 0.204%), the following relation can be used to calculate the diffusion coefficients, D [5]:

$$\frac{c(x,t) - c_0}{c_g - c_0} = \text{erfc}\left(\frac{x}{2 \cdot \sqrt{D \cdot t}}\right) \tag{2}$$

where $x$ is the penetration depth, $t$ the duration of diffusion annealing, and erfc $= 1 -$ erf (erf the Gaussian error function).

In the polycrystalline samples, the tracer diffuses deeper than expected from the volume diffusion. This is due to the effect of grain boundary diffusion. Le Claire [6] proposed the relation between the grain boundary diffusion coefficient and concentration at large depth, which is useful in present case [6]. The value of $(Dt)1/2$ was smaller than the grain size, so the product of oxygen grain boundary coefficient, $D'$ and grain boundary width, $d$, is evaluated as follows:

$$D' \cdot \delta = 0.66(4D/t)^{1/2}\left[-\frac{\partial \log(c(x))}{\partial x^{6/5}}\right]^{-5/3} \tag{3}$$

## 3. Results and Discussion

### 3.1. Bulk Diffusion

Zinc oxide has the wurtzite structure, where the oxygen ions are in hexagonal closed packing. In hexagonal crystals, it is expected that diffusion coefficients for the two principal axes in the basal plane, $D_{xx} = D_{yy}$, is different from $D_{zz}$ in the $c$-axis direction. Figure 1 shows typical depth profiles of $^{18}O$ in single crystals with parallel $(D_{xx})$ and perpendicular $(D_{zz})$ surfaces to the $c$-axis, respectively.

$D_{xx}$ and $D_{zz}$ values are displayed in the Arrenius diagram of Fig. 2. Althouse the values are almost the same as Halling's data, the activation energy of the present study is slightly larger than Halling's [7]. The

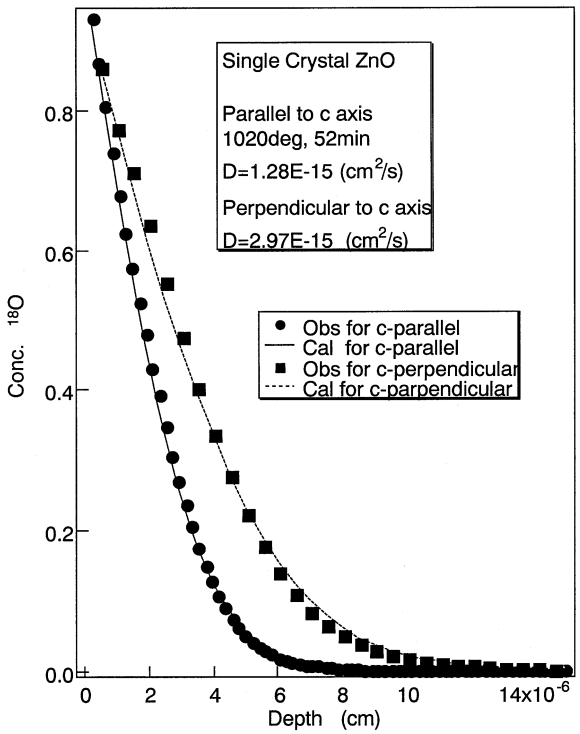


*Fig. 1.* Oxygen 18 diffusion profiles in single crystal zinc oxide. Closed circle and solid line, observed and calculated values for c-parallel direction, respectively. Closed circle and solid line, observed and calculated values for *c*-perpendicular direction, respectively.

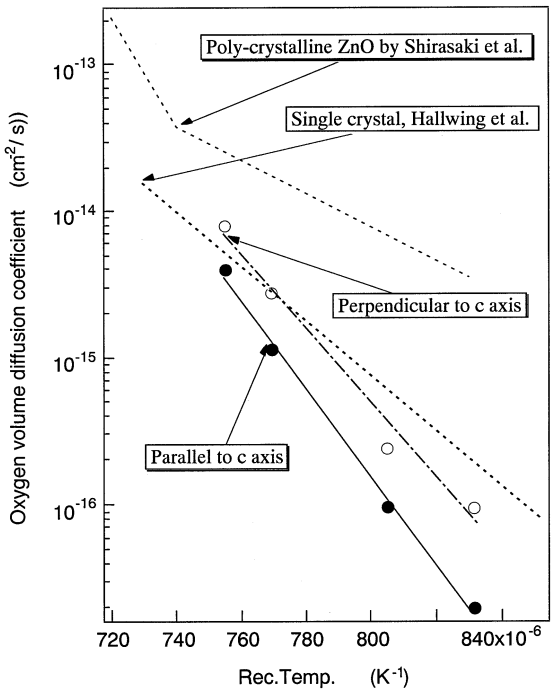


*Fig. 2.* Arrhenius plots for single crystals(present study and Ref [7] and poly crystals Ref [14]).

• and — $D = 1.2\text{E}8 \cdot \exp(-571(\text{kJ/mol})/\text{RT})$: present study.
○ and — $D = 1.5\text{E}5 \cdot \exp(-491(\text{kJ/mol})/\text{RT})$: present study.
— $1350\,\text{K} \leq TD = 3.2\text{E}14 \cdot \exp(-723(\text{kJ/mol})/\text{RT})$ and $1350\,\text{K} \leq TD = 1.3\text{E-}3 \cdot \exp(-267(\text{kJ/mol})/\text{RT})$ (Shirasaki et al., Ref [14])
— $D = 0.6 \cdot \exp(-357(\text{kJ/mol})/\text{RT})$ (Hallwing and Sockel, Ref [7]) □

$D$ values can be represented by two Arrhenius equations, respectively,

$$D = 1.2 \times 10^{8} \cdot \exp(-571(\text{kJ/mol})/\text{RT}) \quad (\text{for } D_{zz}) \quad (4)$$

$$D = 1.5 \times 10^{5} \cdot \exp(-491(\text{kJ/mol})/\text{RT}) \quad (\text{for } D_{xx}) \quad (5)$$

Figure 3 shows a typical depth profile of $^{18}O$ in polycrystalline ZnO samples. The condition of the constant concentration at the surface for a semi-infinite medium was used. The solid line in Fig. 3 indicates the fitted value using data near the surface(< 1000 nm) with a simple error function (Eq. (2)). Lattice diffusion coefficients were obtained, using this equation. The profile had a long tail at larger depth. It is obvious that the long tail was not due to the lattice diffusion but might be caused by the diffusion along grain boundaries. The grain boundary diffusion of oxide ions is discussed later. The lateral distribution of $^{18}O$ ions is shown in Fig. 4, where anisotropy bulk and grain boundary diffusions were observed in polycrystalline samples. It can be possible to evaluate the variation of depth profiles using the same 3-D analysis as shown in Fig. 6(a). In this case, the variation of diffusion coefficients, caused by the anisotropy diffusion, was about 4.

Resultant Arrhenius plots were illustrated in Fig. 5. The lattice diffusion coefficient of oxygen ions depend on the dopants. The Al-doped samples gave the maximum values, and the Li-doped, the minimum values, i.e., the values of the lattice diffusion coefficients with higher valence dopants compare with zinc ions are greater than lower valence dopant such as lithium ions. The values for Al-doped are one to two orders of magnitude larger than Li-doped samples. Thus the variation in bulk diffusion coefficients among samples doped with the various dopants is not caused by anisotropic diffusion, where

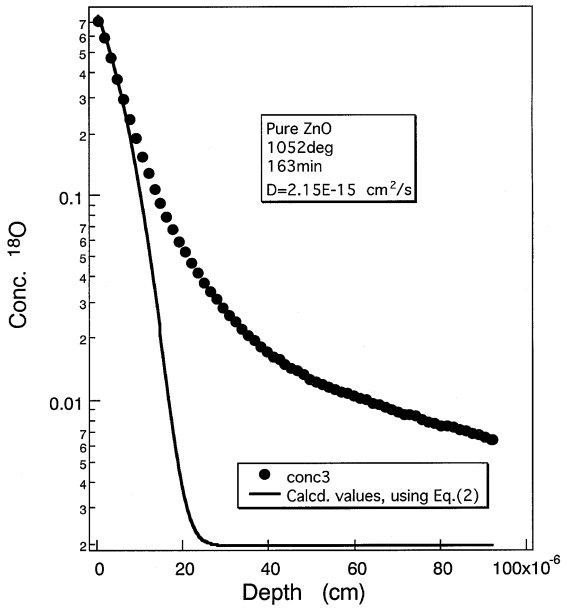


*Fig. 3.* Oxygen 18 depth profile in un-doped ZnO polycrystal, diffusion-annealed at 1052°C for 163 min. Closed circles: observed values. Solid line: calculated values with Eq. (2), assuming only volume diffusion. Discrepancy between the observed and calculated values, indicating the existence of a contribution from the grain boundary diffusion of oxide ions.

the variation factor is less than 4. Accordingly, it might be believed that the oxygen ions diffuse with an interstitialcy mechanism as follows,

Vacancy model:

$$Li_2O \rightarrow 2Li'_{Zn} + O_O^{\times} + V_O^{\cdot\cdot}$$
$$Al_2O_3 + V_O^{\cdot\cdot} \rightarrow 2Al_{Zn}^{\cdot} + 3O_O^{\times}$$

Interstitialcy model:

$$Li_2O + O_i'' \rightarrow 2Li'_{Zn} + 2O_O^{\times}$$
$$Al_2O_3 \rightarrow 2Al_{Zn}^{\cdot} + 2O_O^{\times} + O_i''$$

If the oxygen ions diffuse via oxygen vacancies, then samples doped with Li-ions should have had the highest value. However, Li-doped samples, actually had lower one, reduced values agreeing with the interstitial or interstitialcy mechanism.

A number of oxygen diffusion measurements in ZnO have been performed [7–10]. The various diffusion coefficients are not in particularly good agreement with each other. Because diffusion occurs by extrinsic mechanisms controlled by impurities, such variations are expected. To determine the mechanism, oxygen partial pressure dependent diffusion measurements were done. Moore [8] has claimed a $Po_2$ dependence with exponent $+0.5$ which was discussed in terms of oxygen interstitial migration. On the contrary, Hoffman and Lauder [9] reported values of $-0.5$ and $-1.5$. The negative exponent was considered to be the result of oxygen vacancy diffusion. Our results support the interstitial or interstitilacy mechanism. It is noted that both Moor's data and ours are for polycrystals. Such disagreement would not be unexpected if the defect state was metastable or the diffusion mechanism changed between single and polycrystal ZnO. Furthermore, Robin et al. have claimed that the highest values of Hoffman and Lauder were affected by volatilization of ZnO [10]. Errors due to high vapor pressures of zinc oxides are believed to increase with decreasing oxygen partial pressure.

The diffusion parameters are summarized in Table 1. Although the variation among the results in the polycrystal samples is greater than single crystals and believed to be due to experimental error caused by anisotropic diffusion in polycrysals, there is a tendency that activation energies for single crystals were higher than polycrystals. It is considered that the diffusion mechanism changes from a vacancy one in single crystals to interstitial in polycrystals. The complexity and discrepancy in several results were caused by the mechanism changing, depending on impurity.

### *3.2. Grain Boundary Diffusion*

As seen in Fig. 4(b) of the $^{18}O$ ion image at about 1 $\mu$m depth, the grain boundary network could be observed in pure ZnO. This is considered to be clear evidence of the contribution of grain boundary diffusion to the long tail of diffusion profiles. Same high diffusivities paths along grain boundaries appeared in all samples. Using the data at the tail, one can calculate the product of $D'$ $d$ with Eq. (3). Anisotropic oxygen grain boundary diffusion was also observed. Using RAE-results it is possible to obtain variations with in the same sputtering crater, as shown in Fig. 4. Figure 6(b) shows a typical LeClaire's plots vs. $x^{6/5}$ in Li-doped ZnO annealed at 1052°C. Using the slope in this figure, the values of grain boundary diffusion coefficients were estimated. As seen in Fig. 6(b), the

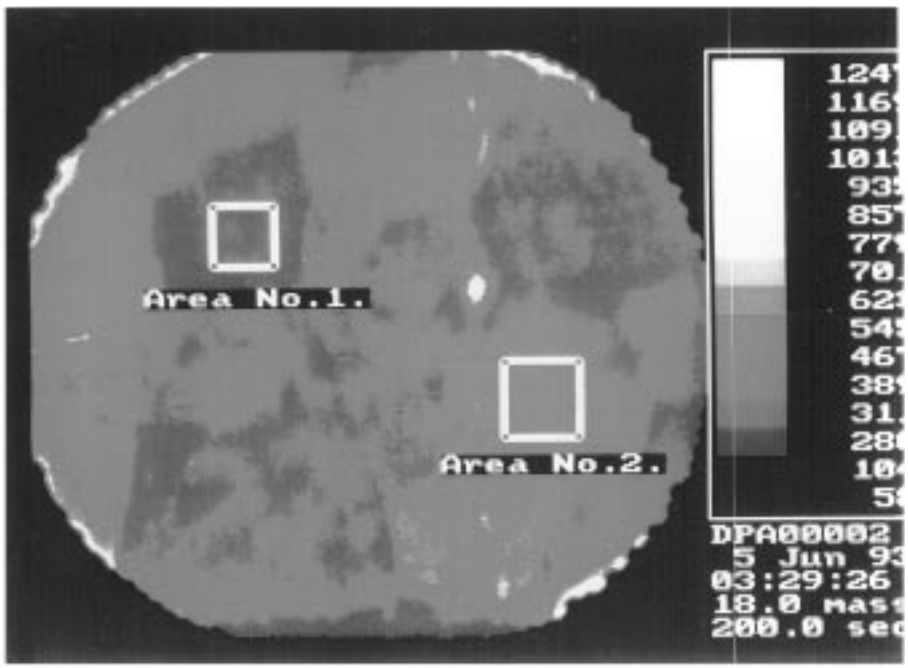


(a)

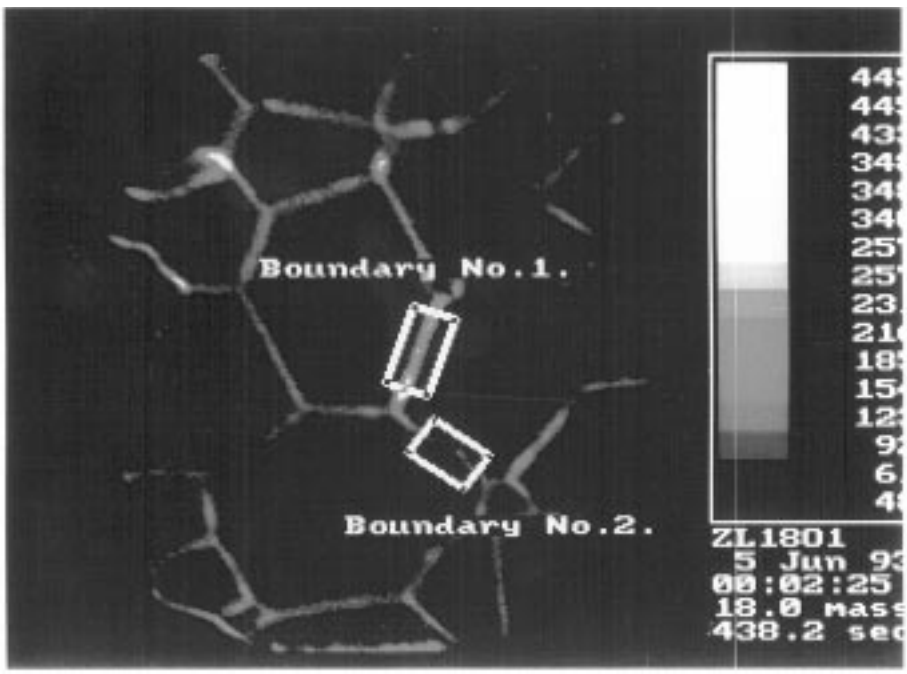


(b)

*Fig. 4.* Two dimensional distribution of Oxygen-18 ions by a planar detector (RAE). (a) Near surface result, being able to obtain the anisotropic behavior of the oxygen volume diffusion. Area No. 1: low diffusivity, $D = 1.27\text{E-}16$ cm2/s, seen in Fig. 6(a). Area No. 2: high diffusivity, $D = 5.13\text{E-}16$cm2/s, seen in Fig. 6(a). (b) $^{18}O$ distribution along grain boundaries at 1 mm depth. Lines; calculated values using Eq. (2). Boundary No. 1: high diffusivity, $dD' = 1.8\text{E-}17$cm3/s, seen in Fig. 6(b). Boundary No. 2: low diffusivity, $dD' = 3.2\text{E-}18$cm3/s, seen in Fig. 6(b). Lines; calculated values using Eq. (3).

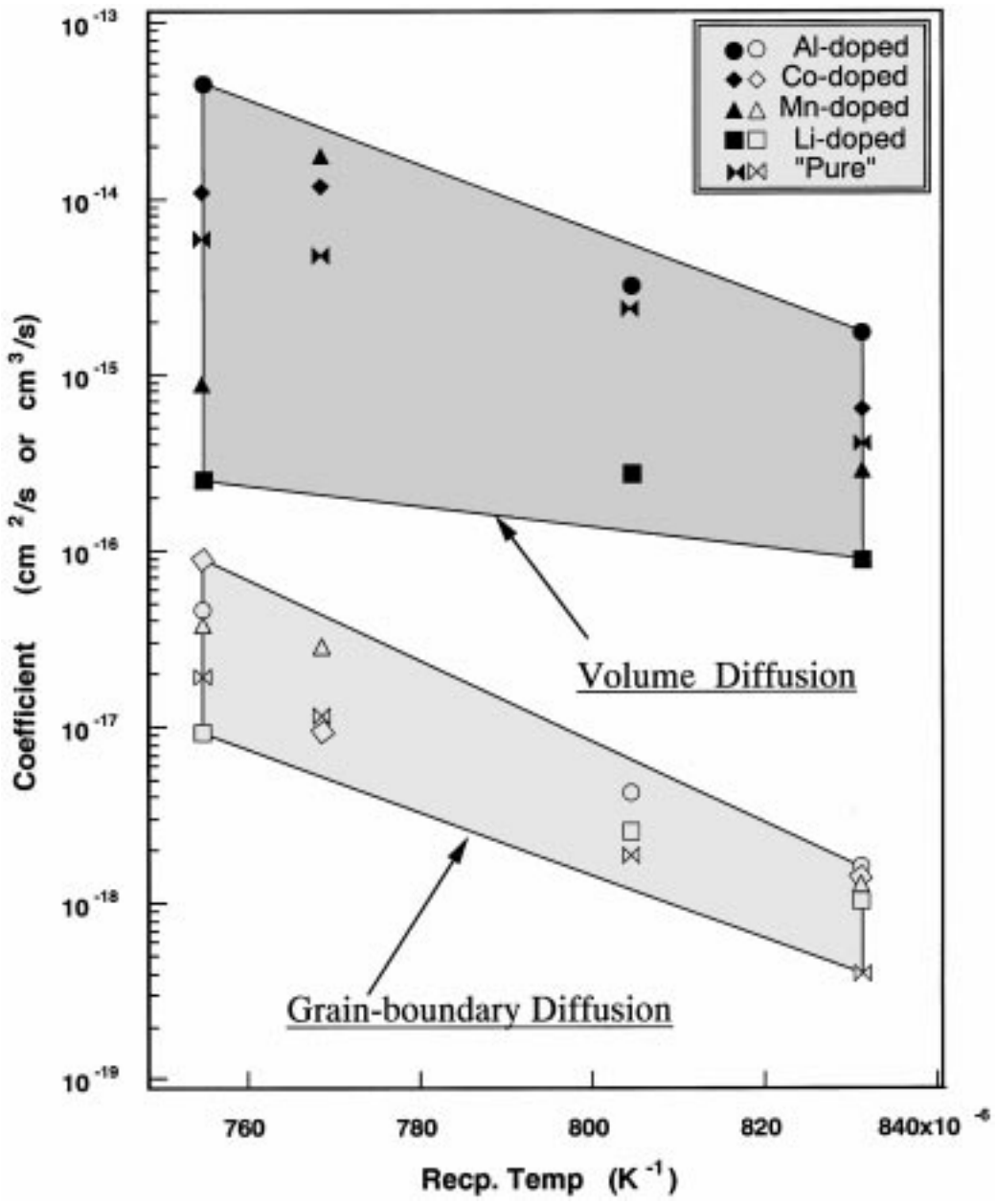


*Fig. 5.* Temperature dependence of oxygen volume diffusion coefficients and grain boundary diffusion coefficients multiplied by $\delta$ in ZnO ceramics.

D value of the high diffusivity grain boundary is one order of magnitude higher than lower one. The product of grain boundary diffusion, $D'$, and boundary width, $\delta$, are also plotted in Fig. 5. The variation of the grain boundary diffusion coefficients was narrower than that for lattice diffusion, indicating that the structure of grain boundaries and mechanism for grain boundary diffusion of oxygen ions depends little on the characteristics of the dopants, and the values only depend on crystalline orientations between two crystals.

The grain boundary and dislocation diffusion are

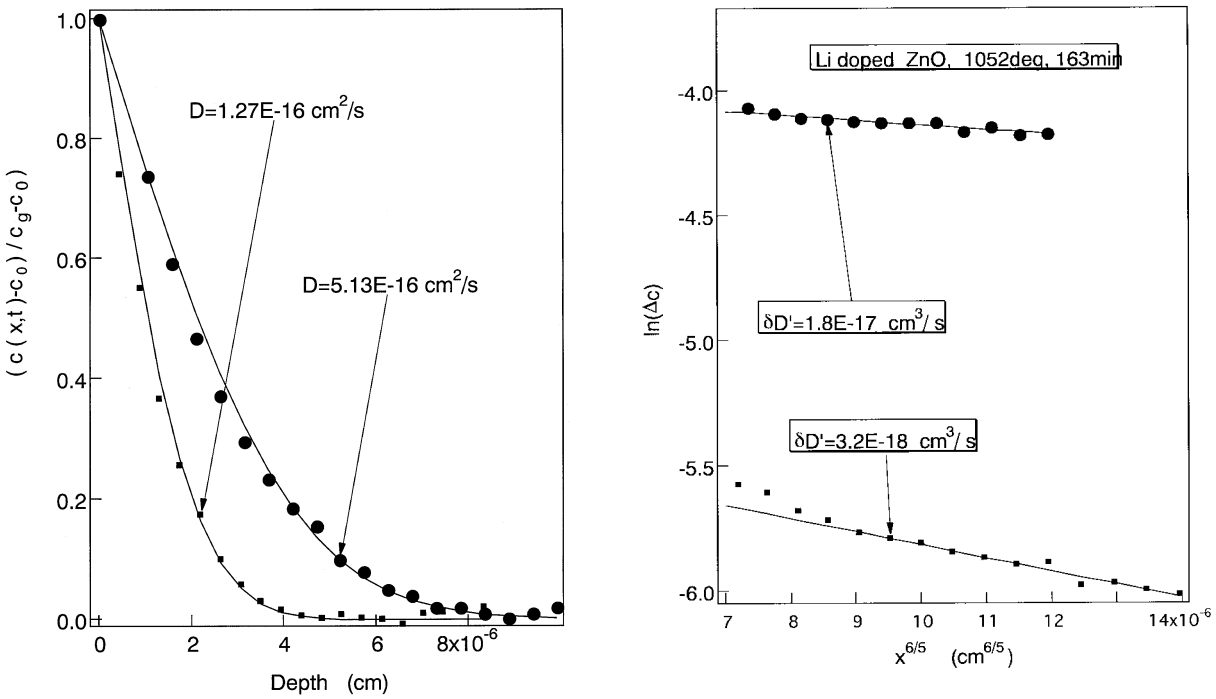


*Fig. 6.* Analysis of oxygen diffusivities, using RAE-3D data. (a) Volume diffusion contribution in Fig. 4(a). Closed squares: low diffusivity, Area No. 1 in Fig. 4(a). Closed circles: high diffusivity, Area No. 2 in Fig. 4(a). (b) Grain boundary diffusion contribution in Fig. 4(b). Closed circles: high diffusivity, Area No. 1 in Fig. 4(b). Closed squares: low diffusivity, Area No. 2 in Fig. 4(b).

considered to follow a pipe diffusion mechanism. Generally, dopants mainly affect the defect concentrations, as influenced by the dopant valences. Since pipe structures have a high density defects, one may suspect that the defect concentration, under these circumstances, is little influenced by aliovalent dopants.

Atkinson et al. [11] have reported the cation self diffusion along grain boundary in nickel oxide and claimed that the width of the boundary, $\delta$, is about $1 \times 10^{-7}$ cm. If the grain boundary width is same order as for cation diffusion in NiO, the grain boundary diffusion coefficient corresponds to the values of four to seven orders of magnitude larger than the lattice diffusion coefficient.

*Table 1.* Oxygen diffusion parameters in single- and polycrystalline zinc oxide

| Sample | $D_o$ (cm$^2$/s) | $\Delta H$ (kJ/mol) |
|---|---|---|
| Single crystal ($\perp$ $c$ axis) | 1.2E8 | $-571 \pm 28$ |
| Single crystal (//$c$ axis) | 1.5E5 | $-491 \pm 50$ |
| Pure (Poly) | 5E-3 | $-298 \pm 91$ |
| Al-doped (Poly) | 7E0 | $-361 \pm 75$ |
| Co-doped (Poly) | 2E-1 | $-332 \pm 77$ |
| Mn-doped (Poly) | E-8 | $-165 \pm 237$ |
| Li-doped (Poly) | 2E-11 | $-123 \pm 27$ |

The varistor characteristics are very sensitive to the type of dopant, and to the preferential oxidation of the grain boundary. The varistor action is lost when ZnO is annealed in a reducing atmosphere. As for the tendency of dopants and annealing-effects, one can think that they are caused by the difference of grain boundary diffusivity of oxide ions. In the present case, only Mn-doped samples behaved as, varistors [12], while the grain boundary diffusirity is believed to be insensitive to the type of dopants. Therefore, the difference of grain boundary diffusion is not the origin of varister action. B: is well known to give a high non-linearity of V-I characteristics [13], which is caused by the existence of excess oxygen at grain boundary. It is noted that oxygen interstitial ions exist, as mentioned above. If the Bi ions are segregating along grain boundaries, the concentration of interstitial oxide ions (excess oxygen ions) is considered to

be increasing. To clarify the varistor mechanism, the diffusion characteristics in Bi-doped ZnO need to be carried out in the future.

## 4. Summary

The characteristics of oxygen diffusion were studied in zinc oxide single and polycrystales. Anisotropic diffusion characteristics were observed in single and polycrystals. The activation energies for single crystals were higher than those of polycrystals. According to the dopant dependence and the variation in the values of the activation energies, the diffusion mechanism in polycrystals was concluded to be interstitial or intersititalcy, and a vacancy mechanism in single crystals.

The grain boundary diffusion characteristics were also evaluated. Anisotropic diffusion was observed as in volume diffusion. The variations in $D_{gb}\delta$ with dopantt was narrower than that for volume diffusion. On this kases,we conclude that the grain boundary is not affected by impurity species but rather by grain boundary structure.

## References

1. G. D. Mahan, L. M. Levinson, and H. R. Philipp, *Appl. Phys. Lett*., **33**, 80 (1978).
2. T. K. Gupta, *J. Am. Cerm. Soc*., **73**, 1817 (1990).
3. Tanaka, Y. Moriyoshi, S. Shirasaki, and T. Yamamoto, in *Hot isostatic pressing: theory and applicatons*, edited by M. Koizumi (Elsevier Science Publications Essex, 1992), p. 105.
4. Y. Oishi and W. D. Kingery, *J. Chem. Phys*., **33**, 905 (1960).
5. J. Crank, in *The Mathematics of Diffusion* (Oxford University Press, London, 1957) P. 30.
6. A. D. Le Claire, *Brit. J. Appl. Phys*., **14**, 351–6 (1963).
7. D. Hallwig and H. G. Sockel, *Reactivity of Solids* (Plenum, New York, 1977) p. 631.
8. W. J. Moore and E. L. Williams, *Disc. Faraday Soc*., **28**, 86 (1959).
9. J. W. Hoffman and J. Lauder, *Trans. Faraday Soc*., **66**, 2346 (1970).
10. R. Robin, A. R. Cooper, and A. H. Heuer, *J. Appl. Phys*., **44**, 3770 (1983).
11. A. Atkinson and R. I. Taylor, *Phil. Mag. A*, **43**, 999–1015 (1981).
12. A. Watanabe, private communication.
13. K. Kostic, O. Milosevic, and D. Uskokovic, Sinter' 85 (1985) p. 301.
14. S. Shirasaki, Y. Moriyoshi, H. Yamamura, H. Haneda, K. Kakegawa, K. Manabe, and M. Ogawa, Zairyo **31**, 850 (1982) (in Japanese).